

SINGLE SIDEBAND MODULATION AS A TOOL TO IMPROVE FUNCTIONAL CONNECTIVITY ESTIMATION

ABSTRACT

Time-resolved functional network connectivity (trFNC) provides a useful tool for representing functional magnetic resonance imaging (fMRI) data with functional networks that change with time. Partly due to its simplicity, sliding window Pearson correlation (SWPC) is the most widely-used method for trFNC estimation. In SWPC, the window size should be selected long enough to avoid spurious estimates of connectivity values, and short enough to capture meaningful fast variations in connectivity estimates. To solve this issue, we propose a method inspired by single sideband (SSB) modulation that allows us to select small window sizes for SWPC without filtering out important low-frequency activity information. We use simulation to show the improvement offered by the proposed method. Additionally, we use fMRI data to show that SSB-SWPC estimates have reduced spurious variation compared with typical SWPC estimators.

Index Terms— time-resolved connectivity, *single-sideband modulation*, fMRI, Pearson correlation, connectivity

1. INTRODUCTION

Functional network connectivity (FNC) collectively refers to the functional relationship between different parts of the brain. As the brain is a dynamic system, it is assumed that FNC changes with time too. Approaches proposed for estimating time-resolved FNC (trFNC) include sliding window Pearson correlation (SWPC) [1], Instantaneous shared trajectory(IST) [2], Filter banked connectivity [3], multiplication of temporal derivatives (MTD)[4], cross wavelet coherence [5]. among many others [6].

SWPC is a widely used method for estimating trFNC partly because of its ease of use. But, like any method, SWPC has its advantages but also several shortcomings [7]. SWPC includes two filters: One highpass filter which is applied to activity time series and one lowpass filter which is applied to connectivity time series. We want to select a window size that is long enough so that the highpass filter does not filter out important low frequency information of activity time series.

But selecting a very large window size will result in a very lowpass connectivity time series and important connectivity information might go undetected. Here we propose a solution to mitigate this issue, allowing us to select smaller window sizes without increasing the amount of spurious estimation.

2. METHODS

2.1. Sliding window Pearson correlation (SWPC)

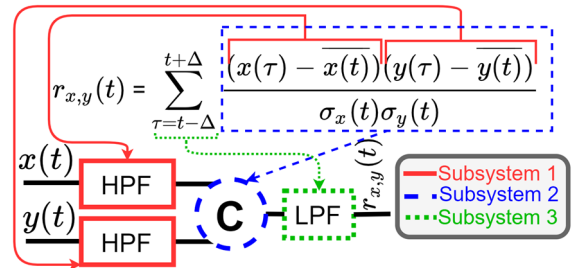


Figure 1. Sliding window Pearson correlation (SWPC) equation and system diagram. SWPC is made of 3 specific subsystems. First, there is a highpass filter (HPF) that is applied to the SWPC input. Then there is a bivariate coupling function C that mixes the information between the filtered activity pairs. Finally, there is a low pass filter (LPF) that is applied to the output of C and gives the connectivity estimate.

Looking at the SWPC equation (Figure 1), we see that it can be broken into three different subsystems: assuming that we have two time series ($x(t)$ and $y(t)$), in the first subsystem (red rectangular part in Figure 1) the sliding average of each of the two time series ($\bar{x}(t)$ and $\bar{y}(t)$ respectively) are removed from the time series. Removing an average of a signal from itself is equivalent to applying a highpass filter (HPF) to the original signal. The second subsystem (blue circle in Figure 1) involving a multiplication (and division by the moving standard deviation) is a coupling function. The final subsystem of SWPC (green rectangular in Figure 1) is simply a moving average function (i.e., low pass filter; LPF). In SWPC, the frequency response of both the HPF and LPF finite impulse response function (FIR) filters are determined by the window length ($2\Delta + 1$) and window shape

(rectangular window in Figure 1). Selecting a higher value for the window length will reduce the cutoff of the HPF which can be considered a desirable selection for the fMRI signal as it is argued that the fMRI signal has a lowpass nature and pre-processing for rsfMRI typically includes a bandpass filter. Because of this, prior studies recommend using longer window sizes up to 100 seconds [7]. One caveat for selecting a longer window size is that $r_{x,y}(t)$ would be very smooth, and as a result, important connectivity variations might go undetected. Note that most research focused on the rsfMRI spectrum applies to the activity time series spectrum and not the connectivity time series spectrum [3].

2.2. Single sideband modulation SWPC (SSB-SWPC)

Inspired by single-sideband (SSB) modulation in communication theory [8] we propose a modification to SWPC which modulates the activity signals ($x(t)$ and $y(t)$) to a higher frequency before passing them through the first HPF subsystem of SWPC. This would allow us to select small window length values without excessively highpass filtering the activity signals. To perform SSB modulation, we first calculate the analytic signals using the Hilbert transform (1) effectively removing the negative part of $x(t)$ spectrum.

$$x_a(t) = x(t) + \sqrt{-1} \times \mathcal{H}[x(t)] \quad (1)$$

Next, we modulate the analytic signal $x_a(t)$ by multiplying it by the term $e^{-i2\pi f_m t}$ and include only the real part of the modulated signal (add the negative part of the spectrum back into the data as real signals have symmetric spectrum).

$$x_m(t) = \text{Re}[x_a(t) \times e^{-i2\pi f_m t}] \quad (2)$$

Figure 2 illustrate these steps. The multiplication in the time domain (the coupling in the SWPC system), is equivalent to circular convolution in the frequency domain.

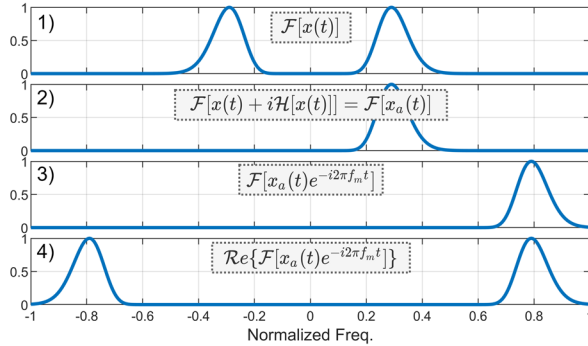


Figure 2. The idea behind SSB. First, the analytic signal is calculated (step 2) removing one sideband of the data. Then this analytic signal is modulated to higher frequencies (step 3) and by calculating the real part of this modulated signal, the other sideband is added back to the spectrum (step 4).

The proposed SSB modulation, will not change the coupling function output (i.e., C in Figure 1) for a specific low-frequency range. Assume that $Z(f)$ and $W(f)$ (the Fourier

transforms of $z(t)$ and $w(t)$) are zero for all frequencies below a specific value (f_{HPF} ; i.e., SWPC HPF cutoff). We also assume that $z_m(f)$ and $w_m(f)$ are the SSB modulated versions of $z(t)$ and $w(t)$ respectively. By thinking about circular convolution visually, we can say that $Z(f) \odot W(f)$ and $Z_m(f) \odot W_m(f)$ are equal for the range:

$$-f_{eq} < f < +f_{eq} \quad (3)$$

$$f_{eq} = \min(2f_{HPF}, f_s - 2(f_m + f_b)) \quad (2)$$

f_s is the sampling frequency, f_m is the modulation value (2) and f_b is the highest frequency that the signals have (signals are bandlimited therefore $f_b \neq f_s$). $2f_{HPF}$ is the shift value where the negative sideband of the signal being shifted overlaps with the positive sideband of the signal being kept in place in the circular convolution. Because frequency transforms of discrete signals are periodic, if we shift the spectrum of one signal by more than $2 \times (f_s/2 - (f_m + f_b))$ the positive sideband of the modulated signal in the range $(-f_s/2, +f_s/2)$ will collide with the negative sideband of the other modulated signal in the range $(+f_s/2, +3f_s/2)$; next period in the spectrum of the signal).

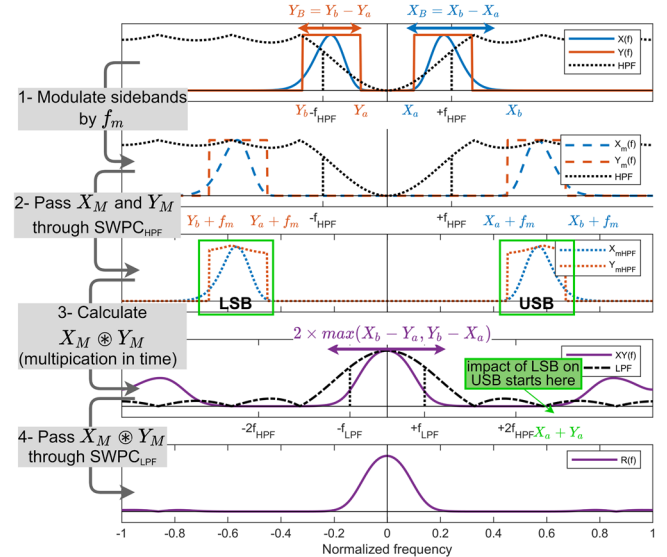


Figure 3 Illustration of the steps in SSB+SWPC. The main reason why SSB improves the SWPC results is seen in step 1. By modulating the signal to higher frequencies (step 1), we make sure that the SWPC highpass filter does not filter any important information of the activity time series. The other steps provide illustrations for the inequalities provided in (4).

Based on step 1 in Figure 3, we can say that $f_m + \min(X_a, Y_a)$ should be higher than f_{HPF} to make sure that HPF part of the signal does not filter out any important low-frequency content. Based on the same step we can see that the modulation should not be so high that aliasing happens. Therefore $f_m + \max(X_b, Y_b)$ should be lower than $f_s/2$ (i.e., Nyquist frequency). Note that essentially $\max(X_b, Y_b)$ is equal to f_b in (3). Based on the step 4 of Figure 3, we can also say that f_{LPF} (LPF cutoff of SWPC) should be lower than

$\max(X_b - Y_a, Y_b - X_a)$ so that we have all the range of possible information on the output. All in all, we can summarize all the inequalities:

$$\begin{aligned} f_m &> f_{HPF} - \min(X_a, Y_a) \\ f_m &< f_s - \max(X_b, Y_b) \\ f_{LPF} &< \min(f_{eq}, \max(X_b - Y_a, Y_b - X_a)) \quad (4) \\ f_{eq} &= \min(2f_{HPF}, f_s - 2(f_m + f_b)) \end{aligned}$$

2.3. Simulation

Here we show how the proposed method improves the estimation of trFNC. Assume that we have two bandlimited time series $x(t)$ and $y(t)$ that we want to have a specific time-resolved covariance matrix $\Sigma_{xy}(t)$. We can achieve this by first generating two independent random signals $x_w(t)$ and $y_w(t)$ by filtering white noise random signals where the filters are determined by the specific bandwidth, we desire for the signals. Next, we can calculate the Cholesky decomposition of $\Sigma_{xy}(t) = L^T L$. Now by using this equation

$$\begin{bmatrix} x(t) \\ y(t) \end{bmatrix} = \begin{bmatrix} x_w(t) \\ y_w(t) \end{bmatrix} L \quad (5)$$

We can have a pair of time series (i.e., $x(t)$ and $y(t)$) that have a covariance of $\Sigma_{xy}(t)$. For this simulation, we chose the sampling frequency to be 2 Hz and the signals to have content in the frequency range [0-0.15] Hz. And for $\Sigma_{xy}(t)$ 1 was selected for the diagonal entries and $0.7\cos(2\pi t \times 0.01)$ in the off-diagonal entries which translate to sinusoidal correlation with a frequency of 0.01 Hz. Additionally, we selected the window size to be equal to 5 time points (3.5 sec). We compared the correlation between the output of typical SWPC and SSB-SWPC proposed here.

2.4. fMRI analysis

To showcase the benefits of the proposed method, we applied SSB+SWPC to a fMRI dataset that includes 314 subjects with TR equal to 2 seconds where the activity is bandpass filtered (0.01-0.15 Hz). After preprocessing steps, a group independent component analysis pipeline (gICA) was applied [1, 9] and 47 components were selected based on their spatial maps. For a more detailed description of the dataset and all the preprocessing and analysis steps see *. For this project, we first upsample the dataset to have a TR of 1 second. This step was performed so that we have a larger frequency range to work with. Next, we estimated pairwise trFNC using both typical SWPC and SSB-SWPC methods using window sizes equal to 7 and 21 time points. Next, to evaluate if the proposed approach improves the estimation of trFNC, we calculated two metrics. The first metric was the mean square difference between the static FNC (FNC calculated over the whole time series temporal range) and averaged trFNC estimated using both SWPC and SSB-SWPC. We predict that as trFNC calculated using SSB modulation is less noisy, its average is closer to sFNC calculated directly. For the second metric, we first concatenated trFNC values across subjects

and time and applied k-means clustering to it based on previous works [1]. Then we calculated dwell time as the number of times points each subject stays in a given cluster. The second metric is the average difference between each subject's dwell time and the window size (i.e., 7 time points). We predict that as SSB+SWPC results in a more robust estimation of trFNC, its dwell times are closer to the SWPC window length. The final results of both methods using 5 clusters and a window size of 7 TR is calculated.

3. RESULTS

Figure 4 shows the simulation results. As can be seen here pairing SSB modulation with SWPC improve the results for almost all values of f_m s for up to 0.15 increase in correlation value (i.e., rho) between estimated trFC and its true value.

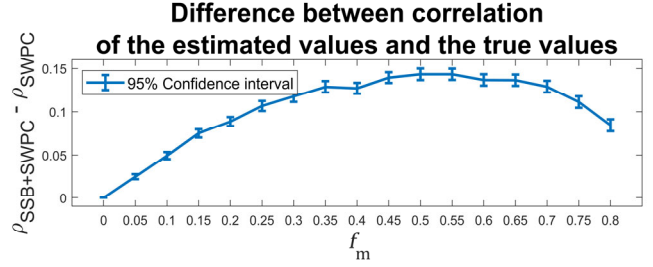


Figure 4. Simulation results. First correlation between connectivity estimation and its true values are calculated for both SSB+SWPC ($\rho_{SSB+SWPC}$) and SWPC (ρ_{SWPC}). Then the difference between these two values is calculated for different modulation values. Results are all positive across different f_m meaning that SSB+SWPC gives a better estimate of the true connectivity time series.

Figure 5 shows the results from the two performance metrics we explained in section 2.4 for both window sizes (7 and 21 TR). As can be seen in this figure, the Mean Square Error (MSE) between sFNC and average trFNC is lower for SSB+SWPC compared to SWPC for both window sizes. Additionally, here we see that SSB+SWPC has resulted in dwell times closer to the window size compared to the classic SWPC result. Collectively, these two observations show that SSB+SWPC results in less spurious trFNC estimates. Figure 6 shows the final clustering for both methods for the window size equal to 7 TR. As can be seen here the cluster centroids (the first two rows) are quite similar for 4 out of 5 clusters. The only cluster that is different is cluster 4. This cluster is not found in higher window sizes for SWPC as reported in [2] and is not reported in any of the other works using the same data that use other methods too *. This leads us to believe that this cluster is the outcome of spurious high-frequency activity portions. This claim needs to be examined in future works. Other clusters have very similar cluster centroids but there are two specific differences in the statistical results of their correspondence dwell time. Namely in cluster 3 SWPC shows a significant difference between the two groups (SZ<HC) while SSB+SWPC does not. On the other

hand, the statistical test for cluster 5 dwell time shows a significant difference between the two groups (SZ>HC) while SWPC only results are not significant. Because of the lack of knowledge about true trFNC states, we cannot say if one cluster is better compared to the other one but it is interesting that cluster 3 (where SWPC results are significant) does not show a lot of modularity (connectivity between all nodes are high here regardless of their functional domains) while cluster 5 (where SSB+SWPC results are significant) shows what looks to be meaningful modularity between domains.

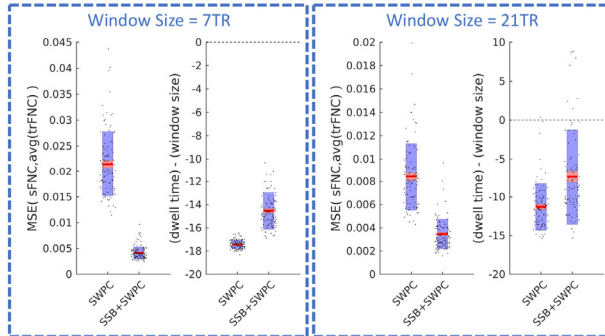


Figure 5. The performance metric of the two methods using two window sizes (one short and one long). The left figure in each of the boxes shows the MSE between sFNC and averaged trFNC resulted from each method. For both window sizes, we see that SSB+SWPC MSE is smaller than SWPC which means that SSB+SWPC is less noisy. Additionally, the right figure in each box shows the average difference between dwell time and the window size used. We can say that the more positive this value the better as we should not be able to find variations smaller than the window sizes. For both window sizes, we see that the SSB+SWPC difference is higher pointing to a less noisy estimation of trFNC.

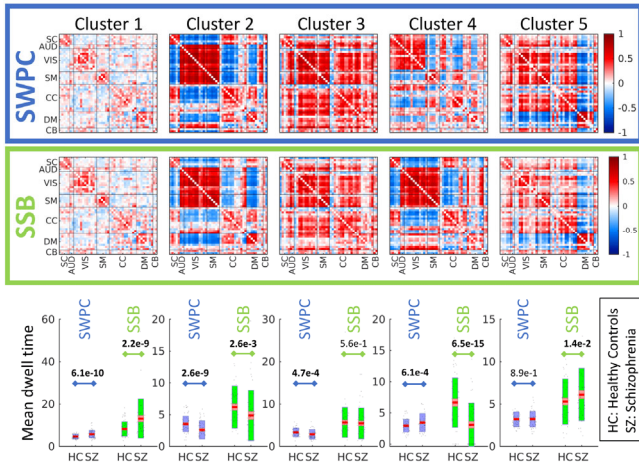


Figure 6. Clustering results of both methods using window size equal to 7 TR.

6. DISCUSSION AND LIMITATION

In this work, we proposed a solution to mitigate one of the major weaknesses of SWPC. Using the idea behind SSB modulation, we move the main content of the activity time series to higher frequencies before calculating trFNC. Using a simple simulation, we showed this method can achieve a better estimate of the connectivity values. Additionally, we showed an application of the proposed SSB+SWPC approach and discussed its SSB+SWPC. We showed how SSB+SWPC can result in dwell time values closer to the window size used and possibly give a more accurate estimation of dwell time. Additionally, we showed how the final results of SSB+SWPC are not significant for a cluster that does not show modularity (which can be argued is not desirable).

There are two specific limitations to the proposed approach: first, this method has additional parameters that need to be selected. Second, SSB+SWPC can result in aliased connectivity values if the users are not knowledgeable enough. To remedy these two limitations, we derived some inequality expressions that give the users a basis for selecting the parameter in addition to avoiding the aliasing issue.

In summary, SSB+SWPC improves the estimation of trFNC allowing us to use smaller window sizes for the SWPC portion without losing the (important) lowpass information in fMRI. This method can also be used to mitigate the limitations of other methods such as IST [2] and MTD [4].

7. REFERENCES

- Allen, E.A., et al.: 'Tracking whole-brain connectivity dynamics in the resting state', *Cereb Cortex*, 2014, 24, (3), pp. 663-676
- Faghiri, A., et al.: 'Weighted average of shared trajectory: A new estimator for dynamic functional connectivity efficiently estimates both rapid and slow changes over time', *Journal of neuroscience methods*, 2020, 334, pp. 108600
- Faghiri, A., et al.: 'A unified approach for characterizing static/dynamic connectivity frequency profiles using filter banks', *Network Neuroscience*, 2021, 5, (1), pp. 56-82
- Shine, J.M., et al.: 'Estimation of dynamic functional connectivity using Multiplication of Temporal Derivatives', *Neuroimage*, 2015, 122, pp. 399-407
- Chang, C., and Glover, G.H.: 'Time-frequency dynamics of resting-state brain connectivity measured with fMRI', *Neuroimage*, 2010, 50, (1), pp. 81-98
- Bolton, T.A., et al.: 'Tapping into multi-faceted human behavior and psychopathology using fMRI brain dynamics', *Trends in Neurosciences*, 2020
- Leonardi, N., and Van De Ville, D.: 'On spurious and real fluctuations of dynamic functional connectivity during rest', *Neuroimage*, 2015, 104, pp. 430-436
- Kschischang, F.R.: 'The hilbert transform', *University of Toronto*, 2006, 83, pp. 277
- Calhoun, V., et al.: 'Independent component analysis applied to fMRI data: a generative model for validating results', *Journal of VLSI signal processing systems for signal, image and video technology*, 2004, 37, (2), pp. 281-291